

Donors and Deep Acceptors in β -Ga₂O₃

Adam T. Neal^{1,a)}, Shin Mou^{1,a)}, Subrina Rafique², Hongping Zhao^{2,3,4}, Elaheh Ahmadi⁵, James S. Speck⁶, Kevin T. Stevens⁷, John D. Blevins⁸, Darren B. Thomson⁸, Neil Moser⁸, Kelson D. Chabak⁸, Gregg H. Jessen⁸

¹ Air Force Research Laboratory, Materials and Manufacturing Directorate, Wright Patterson AFB, OH, 45433, USA

² Department of Electrical Engineering and Computer Science, Case Western Reserve University, Cleveland, OH, 44106, USA

³ Department of Electrical and Computer Engineering, The Ohio State University, Columbus, OH 43210, USA

⁴ Department of Materials Science and Engineering, The Ohio State University, Columbus, OH 43210, USA

⁵ Department of Electrical Engineering and Computer Science, University of Michigan, Ann Arbor, MI, 48103, USA

⁶ University of California, Santa Barbara, Santa Barbara, CA, 93106, USA

⁷ Northrop Grumman SYNOPTICS, Charlotte, NC, 28273, USA

⁸ Air Force Research Laboratory, Sensors Directorate, Wright Patterson AFB, OH, 45433 USA

^{a)} Electronic Address: shin.mou.1@us.af.mil and adam.neal.3@us.af.mil

Abstract

We have studied the properties of Si, Ge shallow donors and Fe, Mg deep acceptors in β -Ga₂O₃ through temperature dependent van der Pauw and Hall effect measurements of samples grown by a variety of methods, including edge-defined film-fed (EFG), Czochralski (CZ), molecular beam epitaxy (MBE), and low pressure chemical vapor deposition (LPCVD). Through simultaneous, self-consistent fitting of the temperature dependent carrier density and mobility, we are able to accurately estimate the donor energy of Si and Ge to be 30 meV in β -Ga₂O₃. Additionally, we show that our measured Hall effect data are consistent with Si and Ge acting as typical shallow donors, rather than shallow DX centers. High temperature Hall effect measurement of Fe doped β -Ga₂O₃ indicates that the material remains weakly n-type even with the Fe doping, with an acceptor energy of 860 meV relative to the *conduction band* for the Fe deep acceptor. Van der Pauw measurements of Mg doped Ga₂O₃ indicate an activation energy of 1.1 eV, as determined from the temperature dependent conductivity.

Excellent performance improvements in Ga₂O₃ power electronics transistors have been made since the first demonstrations of Ga₂O₃ MESFETs¹ and MOSFETs.² Breakdown voltages for Ga₂O₃ Schottky diodes have reached 1.1 kV³ and 1.6 kV,⁴ while breakdown voltages for MOSFETs are as high as 740 V.⁵ Lateral device electric fields of at least 3.8 MV/cm⁶ and vertical device electric fields of 5.1 MV/cm³ have been demonstrated, along with on-currents of 1.5 A/mm.^{7,8} Radio frequency operation of Ga₂O₃ MOSFETs, with f_t and f_{max} as high as 3.3 GHz and 12.9 GHz, respectively, has also been reported.⁹ The rapid pace of Ga₂O₃ device development can be attributed in part to the effective and controllable n-type doping of Ga₂O₃, which has been achieved using tin (Sn),¹⁻¹⁷ silicon (Si),¹⁷⁻²⁴ and, more recently, germanium (Ge),²⁵ consistent with results from DFT calculations.²⁶ Some previous studies have examined the transport properties of shallow donors in Ga₂O₃; however, there remains some discrepancies regarding the energies of the shallow donors. Estimates of the donor energies range from 7.4 meV to 60 meV for Sn,^{2,27,28} 16 meV to 50 meV for Si,²⁹⁻³⁵ and we have previously reported a 17.5 meV donor energy for Ge.³⁶ Recent EPR studies report that Si may also exhibit a DX⁻ state at energy 49 meV;³⁴ however, other groups have reported no evidence for a DX⁻ state.³⁷ In addition to the shallow donor impurities, some impurities have been reported to induce insulating behavior in Ga₂O₃, acting as deep acceptors, including magnesium (Mg)³⁸⁻⁴¹ and iron (Fe).^{42,43}

Given the wide range of donor energies reported in the literature for shallow donors and the limited data available on the deep acceptors, we have undertaken a study to understand the transport properties of Si, Ge, Fe, and Mg doped Ga₂O₃. In the case of shallow donors Si and Ge, by simultaneously and self-consistently fitting both the temperature dependent mobility and temperature dependent carrier density, we are able to accurately determine the donor energy for both Si and Ge to be 30 meV. Additionally, our transport measurements are consistent with Si and

Ge acting as typical shallow donors, rather than shallow DX centers. We also report that EFG grown Fe doped Ga_2O_3 remains weakly n-type, as determined by high temperature Hall effect measurement, with the an acceptor energy for Fe of 0.86 eV relative to the Ga_2O_3 *conduction band*. Finally, we report that the conductivity of CZ grown Ga_2O_3 pulled from a melt with 0.1 mole percent MgO shows an activation energy of 1.1 eV, consistent with the previous report.³⁹

To study the properties of shallow donors in Ga_2O_3 , we have measured and analyzed the temperature dependent carrier density and mobility of several samples determined by van der Pauw and Hall effect measurements in a four terminal configuration. To accurately estimate the donor energies, the carrier density was fit using the charge neutrality equation⁴⁴ and the mobility fit using the solution to the Boltzmann transport equation in the relaxation time approximation,⁴⁵ including the Hall factor,⁴⁶ where ionized impurity,⁴⁷ neutral impurity,⁴⁸ and polar optical phonon⁴⁹ scattering mechanisms were included. An effective mass $m_* = 0.3m_0$,⁵⁰⁻⁵² a low frequency relative dielectric constant $\kappa_S = 10$,^{53,54} a high frequency relative dielectric constant of $\kappa_\infty = 3.5$,⁵⁴⁻⁵⁶ an effective phonon energy $\hbar\omega = 44$ meV,³² and an effective number of phonon modes $M = 1.5$ were used in the calculation. A detailed summary of the relevant equations from the cited references can be found in the supplementary material. Iteration was used to simultaneously and self-consistently fit both the carrier density and mobility. Uncertainty in the compensating acceptor concentration can propagate to the estimated donor energy when fitting the temperature dependent carrier density alone in moderately doped samples. With our approach, we are able to independently determine the compensating acceptor concentration from the ionized impurity limited mobility, allowing for more accurate estimation of the donor energies by avoiding said propagation. Others have used parts of this approach studying the properties of Si doped Ga_2O_3 .³⁰⁻³²

The Si doped samples include a bulk CZ sample from Northrop Grumman Synoptics (Sample 3), a bulk EFG sample from Tamura Corporation (Sample 4), and two epitaxial films grown by LPCVD on c-sapphire substrates with 3.5° (Sample 5) and 6° (Sample 6) offcuts.⁵⁷ Glow discharge mass spectrometry (GDMS) and secondary ion mass spectrometry (SIMS) analysis of EFG Ga₂O₃ samples similar to Sample 4 and SIMS analysis of a CZ grown sample similar to Sample 3 confirm that Si is the dominant unintentional donor in the bulk melt-grown Ga₂O₃ used in this study. Our result is consistent with a previous study which determined that the unintentional Si doping comes from the Ga₂O₃ powder used as the source material for bulk melt-growth.¹⁹ The LPCVD films were intentionally doped using SiCl₄. To make ohmic contacts, four 150 nm Ti/500 nm Au contacts were deposited on the sample edges and annealed in a tube furnace under Ar gas flow up to 450°C. Sample 1 and Sample 2 are Ge doped MBE grown Ga₂O₃ epitaxial films on semi-insulating substrates whose fabrication and growth details are published elsewhere.^{25,36} Figure 1 and Figure 2 show the experimentally measured Hall carrier density and Hall mobility for the samples, along with the temperature dependent fittings. The mobility due to individual scattering mechanisms are shown for Sample 3 only. Parameters of the temperature dependent fittings for the samples are shown in Table I. The donor energies for the samples, along with several samples from the literature, are summarized in Figure 3. As the figure shows, the donor energies for samples seem to converge to a value of 30 meV as the donor concentration approaches 1×10¹⁷ cm⁻³ for both Si and Ge donors. However, as the donor concentration increases above 4×10¹⁷ cm⁻³, the donor energy begins to decrease, as is expected for highly doped semiconductors when an impurity band begins to form.^{58,59} Consistent with this hypothesis, the decrease in the donor energy occurs as the donor density approaches $N_{dn} = (0.2/\alpha)^3 = 1.46 \times 10^{18}$ cm⁻³, where α

is the effective Bohr radius for gallium oxide, which is the estimated density at which a Mott metal-insulator transition would occur for the donor level.^{58,59}

The above analysis assumes that the Si and Ge donors behave as typical shallow donors in Ga₂O₃, but recent EPR measurements have suggested that Si may behave as a shallow DX center.³⁴ By contrast, others have reported that they do not see evidence of DX center behavior in Ga₂O₃.³⁷ To address this open question in light of our Hall effect measurements, let us consider the charge neutrality equation for a DX center⁶⁰

$$N_c \mathcal{F}_{1/2} \left(\frac{E_f - E_c}{kT} \right) + \frac{N_{dn}}{1 + \exp\left(\frac{(2E_{dn} + U) - 2E_f}{kT}\right) + 2 \exp\left(\frac{E_{dn} + U - E_f}{kT}\right)} + N_{ac} = \frac{N_{dn}}{1 + \exp\left(\frac{-(2E_{dn} + U) + 2E_f}{kT}\right) + 2 \exp\left(\frac{-E_{dn} + E_f}{kT}\right)} \quad (1)$$

where N_c is the conduction band effective density of states, N_{ac} the compensating acceptor concentration, N_{dn} the donor concentration, E_{dn} the donor energy, $\mathcal{F}_{1/2}$ the normalized Fermi-Dirac integral of order one half, E_f the Fermi level, and U the interaction energy for two electrons on a single donor. The interaction energy, U , is the energy difference between two electrons on a single donor (DX⁻ state) and two non-interacting electrons on two different donors (neutral state). U is negative, which indicates that the DX⁻ state is the lower energy state, usually due to lattice distortion. For a normal shallow donor, U is a large positive number due to coulomb repulsion of the electrons, and the conventional charge neutrality equation is recovered. Using Equation 1 and the parameters listed in the first two entries of Table II, a comparison of the temperature dependent carrier density and ionized impurity density for the typical normal shallow donor model and the shallow DX donor model are plotted in Figure 4. For the models in Figure 4, values for the normal donor model were chosen to be representative of the experimentally characterized samples listed in Table I, while the values for the DX donor model were chosen to match the temperature dependent carrier density of the normal donor model, with $U = -20$ meV as suggested by the recent EPR study.³⁴ As shown, it is possible to find a set of parameters for the DX donor model

that almost match the temperature dependent carrier density of the normal donor model; however, as the dashed lines show, the density of ionized impurities at low temperatures is about a factor of five larger for the DX donor model. Because the density of ionized impurities is so much larger for the DX donor model, it underestimates the experimentally measured mobility of our samples at low temperatures where ionized impurity scattering dominates, as shown in Figure 5, with fitting parameters shown in Table II. This fact means that the DX donor model cannot be used to fit our measured Hall mobility and carrier density data. This analysis assumes that the spatial distribution of donors in the negatively charged DX^- state and those in the typical positively charged ionized state are uncorrelated, so that all donors act as point-charge-like scattering centers. However, there is some evidence that the distributions of DX^- donors and positively charged ionized donors can become correlated, acting as weaker dipole-like scattering centers.⁶¹ While such a correlation may partially account for the discrepancy between our measured mobility data and the DX donor mobility models presented in Figure 5, it does not fully account for the factor of 4 to 5 discrepancy in low temperature mobility for Si doped Sample 3 and Sample 4. Therefore, our measured Hall data for these Si doped samples are consistent with a normal shallow donor and are inconsistent with a shallow DX center. This observation agrees with Irmscher et al.,³⁷ who also reports no evidence of DX behavior. We note, however, that we are only able to rule out DX center behavior in our samples because they have a compensation ratio N_{ac}/N_{dn} less than one third. For compensation ratios of one third or greater in the normal donor model, it is always possible to find a set of parameters for the DX donor model that match both the temperature dependent carrier density and the low temperature ionized impurity density. This fact means that a normal shallow donor and shallow DX donor can only be distinguished using simultaneous, self-consistent carrier density and mobility fitting for compensation ratios less than one third, as is the case here.

Considering the remarkable consistency in experimental results across a wide variety of growth methods, including EFG, CZ, MBE, and LPCVD, along with the fact that Si and Ge are both group IV elements on the periodic table, we can conclude that Si and Ge act as typical shallow donors in all of the samples presented here.

In addition to measurements on Si and Ge donor doped samples, we have characterized Fe and Mg acceptor doped samples as well using the same four terminal van der Pauw and Hall effect measurement techniques. Due to the semi-insulating nature of these samples, high temperature Hall effect measurements were necessary to thermally activate carriers to enable Hall effect measurement. Measurements were performed under N₂ gas flow in a tube furnace with an external silicon carbide heater and electromagnet. Figure 6 shows the Hall carrier density for an Fe doped, EFG grown semi-insulating substrate from Tamura Corporation (Sample 7). Hall effect measurement was possible for temperatures above 400 K, with the sign of the Hall effect indicating that the β -Ga₂O₃ remains weakly n-type at elevated temperatures even with Fe doping. Glow discharge mass spectrometry analysis (GDMS) performed on a similar Fe doped sample indicates a concentration of about $1 \times 10^{17} \text{ cm}^{-3}$ for the unintentional Si donor and $8 \times 10^{17} \text{ cm}^{-3}$ for the intentional Fe acceptor. Therefore, we ascribe the observed n-type behavior to thermal activation of electrons on ionized Fe acceptors into the conduction band. Fitting with the charge neutrality equation yields an acceptor energy $E_c - E_{ac}$ of 860 meV. Note that this acceptor energy is referenced to the conduction band edge due to the n-type behavior. This acceptor energy near the conduction band is consistent with preliminary DFT calculations of Fe doped Ga₂O₃ which indicate that Fe induces midgap states closer to the conduction band.⁴³ The acceptor energy is somewhat higher than that recently observed via DLTS for Fe impurities in n-type bulk substrates,⁶² however, this difference can be explained by the broadening of the Fe acceptor energy

level at the much higher Fe concentration in this semi-insulating substrate. Because the carrier density does not saturate at higher temperatures, it is not possible to estimate the absolute value of the Fe and Si concentrations in this sample. However, the ratio of Fe acceptors to Si donors, N_{ac}/N_{dn} , is uniquely determined to be 1.65 by fitting the temperature dependent carrier density using the charge neutrality equation. We note that this ratio is smaller than one would expect based on the GDMS results, which could suggest that not all of the Fe dopants in the sample are electrically active. Finally, the inset of Figure 6 shows the temperature dependent conductivity measured by the van der Pauw method for an Mg doped sample grown by Northrop Grumman Synoptics using the CZ method (Sample 8). The melt from which the sample was pulled contained 0.1 mole % of MgO. Hall effect measurement was attempted, but it was not possible to resolve the Hall voltage due to low signal to noise ratio as a result of the very low conductivity for the sample. Least squares fitting of the temperature dependent conductivity indicates an empirical activation energy of 1.1 eV, which is consistent with a previous report on the activation energy of highly Mg doped Ga₂O₃.³⁹ Because Si contamination is present in these CZ grown samples, it is expected that the activation energy of 1.1 eV is approximately equal to the acceptor energy for Mg. However, without Hall effect measurement, it is not possible to determine the carrier type of the Mg doped sample. This fact means that we are unable to determine if this 1.1 eV activation energy is referenced to the conduction band or valence band edge of Ga₂O₃ from experiment, although recent DFT studies indicate the Mg acceptor level is closer to the valence band.⁶³

In conclusion, simultaneous, self-consistent fitting of the temperature dependent carrier density and mobility of n-type β -Ga₂O₃, as measured by the van der Pauw and Hall effect methods, indicates a donor ionization energy of 30 meV for Si and Ge shallow donors. Accurate determination of the donor energy is enabled by reliable estimation of the compensating acceptor

concentration through fitting of the low temperature ionized impurity limited mobility. Additionally, comparison of our Hall effect data to appropriate models indicates that Si and Ge act as typical shallow donors in the β -Ga₂O₃ samples presented here, as opposed to shallow DX centers. Finally, Fe doped β -Ga₂O₃ is shown to remain weakly n-type by high temperature Hall effect measurements, with an acceptor energy of 860 meV relative to the Ga₂O₃ *conduction band*.

Supplementary Material

See supplementary material for a summary of the relevant equations from the cited references used to fit the temperature dependent carrier density and mobility data.

Acknowledgements

The material is partially based upon the work supported by the Air Force Office of Scientific Research under award number FA9550-18RYCOR098. J.S.S. was also supported by the Defense Threat Reduction Agency through program HDTRA-17-1-0034. The content of the information does not necessarily reflect the position or the policy of the federal government, and no official endorsement should be inferred.

References

- ¹ M. Higashiwaki, K. Sasaki, A. Kuramata, T. Masui, and S. Yamakoshi, *Appl. Phys. Lett.* **100**, 013504 (2012).
- ² M. Higashiwaki, K. Sasaki, T. Kamimura, M.H. Wong, D. Krishnamurthy, A. Kuramata, T. Masui, and S. Yamakoshi, *Appl. Phys. Lett.* **103**, 123511 (2013).
- ³ K. Konishi, K. Goto, H. Murakami, Y. Kumagai, A. Kuramata, S. Yamakoshi, and M. Higashiwaki, *Appl. Phys. Lett.* **110**, 103506 (2017).
- ⁴ J. Yang, S. Ahn, F. Ren, S.J. Pearton, S. Jang, and A. Kuramata, *IEEE Electron Device Lett.* **38**, 906 (2017).
- ⁵ M.H. Wong, K. Sasaki, A. Kuramata, S. Yamakoshi, and M. Higashiwaki, *IEEE Electron Device Lett.* **37**, 212 (2016).
- ⁶ A.J. Green, K.D. Chabak, E.R. Heller, R.C. Fitch, M. Baldini, A. Fiedler, K. Irmscher, G. Wagner, Z. Galazka, S.E. Tetlak, A. Crespo, K. Leedy, and G.H. Jessen, *IEEE Electron Device Lett.* **37**, 902 (2016).

- ⁷ H. Zhou, M. Si, S. Alghamadi, G. Qiu, L. Yang, and P.D. Ye, *IEEE Electron Device Lett.* **38**, 103 (2017).
- ⁸ H. Zhou, K. Maize, G. Qiu, A. Shakouri, and P.D. Ye, *Appl. Phys. Lett.* **111**, 092102 (2017).
- ⁹ A.J. Green, K.D. Chabak, M. Baldini, N. Moser, R. Gilbert, R.C. Fitch, G. Wagner, Z. Galazka, J. McCandless, A. Crespo, K. Leedy, and G.H. Jessen, *IEEE Electron Device Lett.* **38**, 790 (2017).
- ¹⁰ N. Ueda, H. Hosono, R. Waseda, and H. Kawazoe, *Appl. Phys. Lett.* **70**, 3561 (1997).
- ¹¹ J. Zhang, C. Xia, Q. Deng, W. Xu, H. Shi, F. Wu, and J. Xu, *J. Phys. Chem. Solids* **67**, 1656 (2006).
- ¹² N. Suzuki, S. Ohira, M. Tanaka, T. Sugawara, K. Nakajima, and T. Shishido, *Phys. Status Solidi C* **4**, 2310 (2007).
- ¹³ K. Sasaki, A. Kuramata, T. Masui, E.G. Vllora, K. Shimamura, and S. Yamakoshi, *Appl. Phys. Express* **5**, 035502 (2012).
- ¹⁴ W. Mi, X. Du, C. Luan, H. Xiao, and J. Ma, *RSC Adv.* **4**, 30579 (2014).
- ¹⁵ D. Gogova, M. Schmidbauer, and A. Kwasniewski, *CrystEngComm* **17**, 6744 (2015).
- ¹⁶ M. Baldini, M. Albrecht, A. Fiedler, K. Irmischer, D. Klimm, R. Schewski, and G. Wagner, *J. Mater. Sci.* **51**, 3650 (2016).
- ¹⁷ M. Baldini, M. Albrecht, A. Fiedler, K. Irmischer, R. Schewski, and G. Wagner, *ECS J. Solid State Sci. Technol* **6**, Q3040 (2017).
- ¹⁸ E.G. Vllora, K. Shimamura, Y. Yoshikawa, T. Ujiie, and K. Aoki, *Appl. Phys. Lett.* **92**, 202120 (2008).
- ¹⁹ A. Kuramata, K. Koshi, S. Watanabe, Y. Yamaoka, T. Masui, and S. Yamakoshi, *Jpn. J. Appl. Phys.* **55**, 1202A2 (2016).
- ²⁰ D. Gogova, G. Wagner, M. Baldini, M. Schmidbauer, K. Irmischer, R. Schewski, and Z. Galazka, *J. Cryst. Growth* **401**, 665 (2014).
- ²¹ S. Rafique, L. Han, A.T. Neal, S. Mou, M.J. Tadjer, R.H. French, and H. Zhao, *Appl. Phys. Lett.* **109**, 132103 (2016).
- ²² M. Higashiwaki, K. Sasaki, K. Goto, K. Nomura, Q.T. Thieu, R. Togashi, H. Murakami, Y. Kumagai, B. Monemar, A. Koukitu, A. Kuramata, and S. Yamakoshi, in *73rd Annual Device Research Conference (DRC)*, Columbus, Ohio, 21 June 2015, pp. 29-30
- ²³ M. Higashiwaki, K. Konishi, K. Sasaki, K. Goto, K. Nomura, Q.T. Thieu, R. Togashi, H. Murakami, Y. Kumagai, B. Monemar, A. Koukitu, A. Kuramata, and S. Yamakoshi, *Appl. Phys. Lett.* **108**, 133503 (2016).
- ²⁴ S. Krishnamoorthy, Z. Xia, S. Bajaj, M. Brenner, and S. Rajan, *Appl. Phys. Express* **10**, 051102 (2017).
- ²⁵ E. Ahmadi, O.S. Koksaldi, S.W. Kaun, Y. Oshima, D.B. Short, U.K. Mishra, and J.S. Speck, *Appl. Phys. Express* **10**, 041102 (2017).
- ²⁶ J.B. Varley, J.R. Weber, A. Janotti, and C.G. Van de Walle, *Appl. Phys. Lett.* **97**, 142106 (2010).
- ²⁷ M. Orita, H. Ohta, and M. Hirano, *Appl. Phys. Lett.* **77**, 4166 (2000).
- ²⁸ T. Oishi, K. Harada, Y. Koga, and M. Kasu, *Jpn. J. Appl. Phys.* **55**, 030305 (2016).

- ²⁹ K. Irmscher, Z. Galazka, M. Pietsch, R. Uecker, and R. Fornari, *J. Appl. Phys.* **110**, 063720 (2011).
- ³⁰ A. Parisini and R. Fornari, *Semicond. Sci. Technol* **31**, 035023 (2016).
- ³¹ T. Oishi, Y. Koga, K. Harada, and M. Kasu, *Appl. Phys. Express* **8**, 031101 (2015).
- ³² N. Ma, N. Tanen, A. Verma, Z. Guo, T. Luo, H.G. Xing, and D. Jenna, *Appl. Phys. Lett.* **109**, 212101 (2016).
- ³³ A.T. Neal, S. Mou, R. Lopez, J.V. Li, D.B. Thomson, K.D. Chabak, and G.H. Jessen, *Sci. Rep.* **7**, 13218 (2017).
- ³⁴ N.T. Son, K. Goto, K. Nomura, Q.T. Thieu, R. Togashi, H. Murakami, Y. Kumagai, A. Kuramata, M. Higashiwaki, A. Koukitu, S. Yamakoshi, B. Monemar, and E. Janzén, *J. Appl. Phys.* **120**, 235703 (2016).
- ³⁵ M. Higashiwaki, A. Kuramata, H. Murakami, and Y. Kumagai, *J. Phys. D* **50**, 333002 (2017).
- ³⁶ N. Moser, J. McCandless, A. Crespo, K. Leedy, A. Green, A. Neal, S. Mou, E. Ahmadi, J. Speck, K. Chabak, N. Peixoto, and G. Jessen, *IEEE Electron Device Lett.* **38**, 775 (2017).
- ³⁷ K. Irmscher, in *2nd International Workshop on Ga₂O₃ and Related Materials*, Parma, Italy, 2017, p. I5
- ³⁸ T. Onuma, S. Fujioka, T. Yamaguchi, M. Higashiwaki, K. Sasaki, T. Masui, and T. Honda, *Appl. Phys. Lett.* **103**, 041910 (2013).
- ³⁹ T. Harwig and J. Schoonman, *J. Solid State Chem.* **23**, 205 (1978).
- ⁴⁰ M.H. Wong, K. Goto, A. Kuramata, S. Yamakoshi, H. Murakami, Y. Kumagai, and M. Higashiwaki, in *75th Device Research Conference*, South Bend, IN, USA, 2017, p. 7999413
- ⁴¹ C. Tang, J. Sun, N. Lin, Z. Jia, W. Mu, X. Tao, and X. Zhao, *RSC Adv.* **6**, 78322 (2016).
- ⁴² M.H. Wong, K. Sasaki, A. Kuramata, S. Yamakoshi, and M. Higashiwaki, *Appl. Phys. Lett.* **106**, 032105 (2015).
- ⁴³ H. He, W. Li, H.Z. Xing, and E.J. Liang, *Adv. Mat. Res.* **535-537**, 36 (2012).
- ⁴⁴ S.M. Sze and K.K. Ng, *Physics of Semiconductor Devices*, 3rd ed. (John Wiley & Sons, 2007) pp. 17-27
- ⁴⁵ M. Lundstrom, *Fundamentals of Carrier Transport 2nd ed.* (Cambridge University Press, New York, 2000) pp. 136-137
- ⁴⁶ M. Lundstrom, *Fundamentals of Carrier Transport 2nd ed.* (Cambridge University Press, New York, 2000) p. 171
- ⁴⁷ M. Lundstrom, *Fundamentals of Carrier Transport 2nd ed.* (Cambridge University Press, New York, 2000) p. 70
- ⁴⁸ C. Erginsoy, *Phys. Rev.* **79**, 1013 (1950).
- ⁴⁹ M. Lundstrom, *Fundamentals of Carrier Transport 2nd ed.* (Cambridge University Press, New York, 2000) p. 86
- ⁵⁰ H. He, R. Orlando, M.A. Blanco, R. Pandey, E. Amzallag, I. Baraille, and M. Rérat, *Phys. Rev. B* **74**, 195123 (2006).
- ⁵¹ H. Peelaers and C.G. Van de Walle, *Phys. Status Solidi B* **252**, 828 (2015).
- ⁵² J. Furthmüller and F. Bechstedt, *Phys. Rev. B* **93**, 115204 (2016).
- ⁵³ B. Hoeneisen, C.A. Mead, and M.A. Nicolet, *Solid-State Electron.* **14**, 1057 (1971).

- ⁵⁴ M. Schubert, R. Korlacki, S. Knight, T. Hofmann, S. Schöche, V. Darakchieva, E. Janzén, B. Monemar, D. Gogova, Q.-T. Thieu, R. Togashi, H. Murakami, Y. Kumagai, K. Goto, A. Kuramata, S. Yamakoshi, and M. Higashiwaki, *Phys. Rev. B* **93**, 125209 (2016).
- ⁵⁵ M. Rebien, W. Henrion, M. Hong, J.P. Mannaerts, and M. Fleischer, *Appl. Phys. Lett.* **81**, 250 (2002).
- ⁵⁶ C. Sturm, J. Furthmuller, F. Bechstedt, R. Schmidt-Grund, and M. Grundmann, *APL Mater.* **3**, 106106 (2015).
- ⁵⁷ S. Rafique, L. Han, A.T. Neal, S. Mou, J. Boeckl, and H. Zhao, *Phys. Status Solidi A* **215**, 1700467 (2018).
- ⁵⁸ E.M. Conwell, *Phys. Rev.* **103**, 51 (1956).
- ⁵⁹ N.F. Mott, *Rev. Mod. Phys.* **40**, 677 (1968).
- ⁶⁰ D.C. Look, *Phys. Rev. B* **24**, 5852 (1981).
- ⁶¹ E.P. O'Reilly, *Appl. Phys. Lett.* **55**, 1409 (1989).
- ⁶² M.E. Ingebrigtsen, J.B. Varley, A.Y. Kuznetsov, B.G. Svensson, G. Alfieri, A. Mihaila, U. Badstübner, and L. Vines, *Appl. Phys. Lett.* **112**, 042104 (2018).
- ⁶³ A. Kyrtsos, M. Matsubara, and E. Bellotti, *Appl. Phys. Lett.* **112**, 032108 (2018).

Table I: Parameters of temperature dependent carrier density and mobility fitting for n-type β -Ga₂O₃ samples

	Growth Method	Dopant	N_{dn} 10 ¹⁶ cm ⁻³	E_{dn} ^a meV	N_{ac} 10 ¹⁶ cm ⁻³	N_{ac}/N_{dn}	$N_{neutral}$ ^b 10 ¹⁶ cm ⁻³	$\hbar\omega$ ^c meV
Sample 1 ^d	MBE	Ge	6.5	28	4.8	0.74	80	44
Sample 2	MBE	Ge	30	29	3.9	0.13	80	44
Sample 3	CZ	Si	13	30	0.91	0.07		44
Sample 4	EFG	Si	30	27	1.5	0.05		44
Sample 5	LPCVD	Si	80	19	5.6	0.07	100	44
Sample 6	LPCVD	Si	100	15	5.0	0.05		44
Fornari et al. #12 ^e	CZ	Si	14.3	28.5	4.2			
Fornari et al. #3 ^e	CZ	Si	48.3	21.2	14			
Fornari et al. #7 ^e	CZ	Si	61.7	24.9	5.4			
Oishi et al. ^f	EFG	Si	14	31	2.7			

^a Referenced to conduction band, ^b Additional neutral impurities beyond unionized donors

^c Ref. 32, ^d A 2nd donor with $E_{dn2} = 100$ meV and $N_{dn2} = 1.5 \times 10^{16}$ cm⁻³ was also included³³

^e Refs. 29,30 ^f Ref. 31

Table II: Parameters for Comparing Normal Donor and DX Donor models

	N_{dn} 10 ¹⁶ cm ⁻³	E_{dn} meV	U meV	N_{ac} 10 ¹⁶ cm ⁻³	N_{ac}/N_{dn}
Normal Fig. 4	11	30	$+\infty$	1.1	0.1
DX Fig. 4	10	16	-20	0	0
Sample 2 DX, Fig. 5	27	16	-10	5.4	0.2
Sample 3 DX, Fig. 5	13	18	-10	0	0
Sample 4 DX, Fig. 5	25	10	-15	0	0

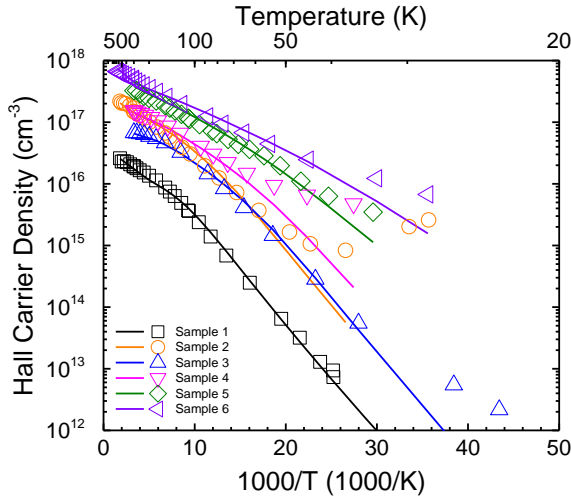


Figure 1: Measured Hall carrier density (symbols) and fittings (solid lines) for Si and Ge doped β - Ga_2O_3 samples.

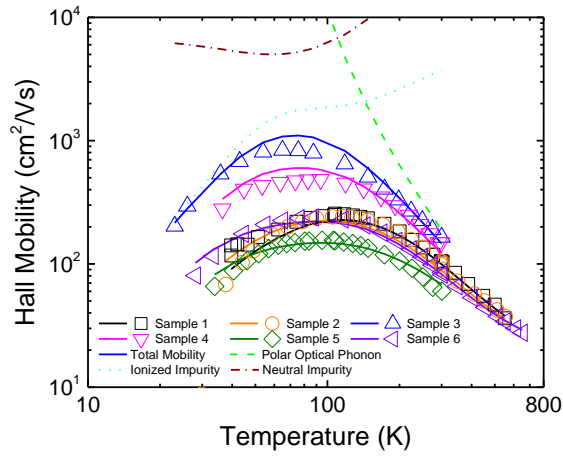


Figure 2: Measured Hall mobility (symbols) and fittings (solid lines) for Si and Ge doped β - Ga_2O_3 samples. Individual components of the mobility are shown for Sample 3, with the scattering mechanisms indicated in the legend.

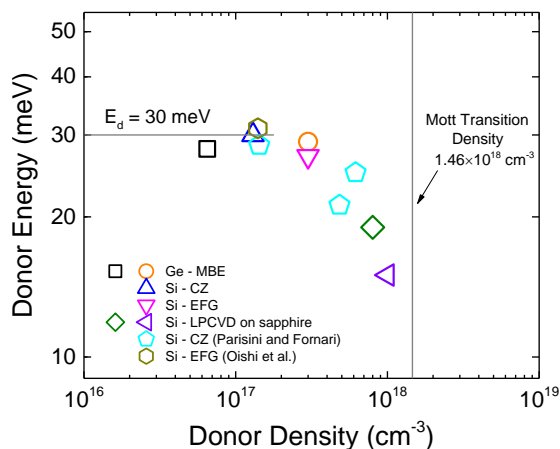


Figure 3: Summary of the donor energies as a function of donor concentration. Data from the literature^{30,31} are also included as indicated in the figure legend.

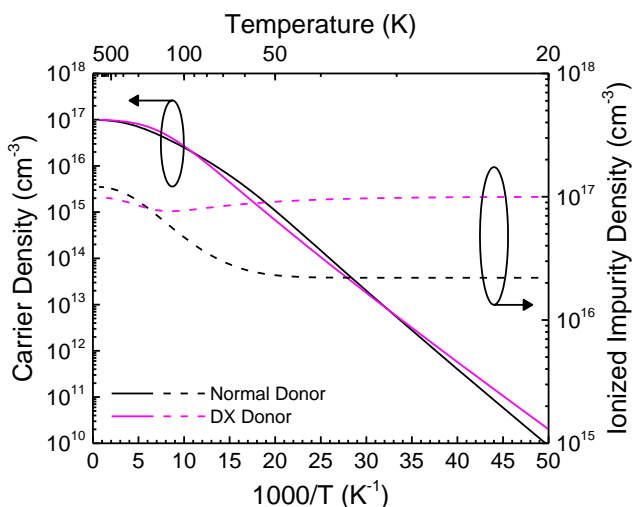


Figure 4: Comparison of carrier density and ionized impurity density vs. temperature for a normal donor and a DX center with $N_{dn} - N_{ac}$ of $1 \times 10^{17} \text{ cm}^{-3}$. Other parameters for the two models are shown in Table II. The higher concentration of ionized impurities at low temperature in the DX donor model leads to underestimation of the experimentally measured Hall mobility as shown in Figure 5.

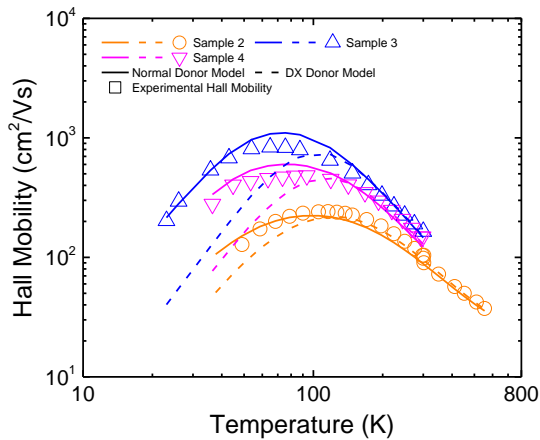


Figure 5: Comparison of mobility fitting using the normal donor model (solid lines) and the DX donor model (dashed lines) to the experimentally measured Hall mobility for Sample 2, Sample 3, and Sample 4. Only the normal donor model can fit the experimental data, as the DX donor model yields too much ionized impurity scattering at low temperatures and underestimates the experimentally measured mobility.

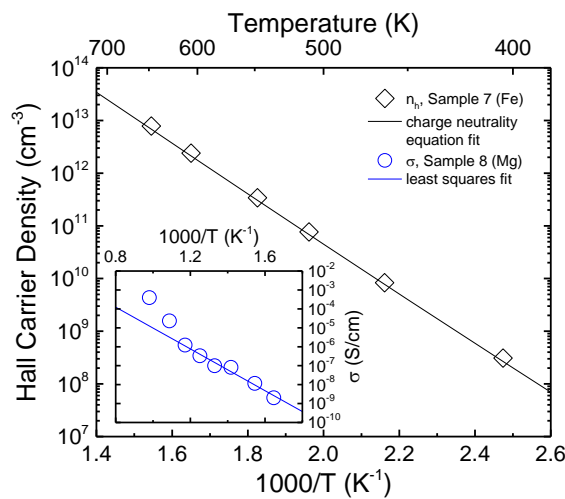


Figure 6: High temperature Hall carrier density for Sample 7, an Fe doped semi-insulating β - Ga_2O_3 sample. The sign of the Hall effect indicates that the sample is weakly n-type at elevated temperatures. Inset: Temperature dependent conductivity of Sample 8, an Mg doped semi-insulating β - Ga_2O_3 sample.

Supplementary Material: Donors and Deep Acceptors in β -Ga₂O₃

Adam T. Neal^{1,a)}, Shin Mou^{1,a)}, Subrina Rafique², Hongping Zhao^{2,3,4}, Elaheh Ahmadi⁵, James S. Speck⁶, Kevin T. Stevens⁷, John D. Blevins⁸, Darren B. Thomson⁸, Neil Moser⁸, Kelson D. Chabak⁸, Gregg H. Jessen⁸

¹ Air Force Research Laboratory, Materials and Manufacturing Directorate, Wright Patterson AFB, OH, 45433, USA

² Department of Electrical Engineering and Computer Science, Case Western Reserve University, Cleveland, OH, 44106, USA

³ Department of Electrical and Computer Engineering, The Ohio State University, Columbus, OH 43210, USA

⁴ Department of Materials Science and Engineering, The Ohio State University, Columbus, OH 43210, USA

⁵ Department of Electrical Engineering and Computer Science, University of Michigan, Ann Arbor, MI, 48103, USA

⁶ University of California, Santa Barbara, Santa Barbara, CA, 93106, USA

⁷ Northrop Grumman SYNOPTICS, Charlotte, NC, 28273, USA

⁸ Air Force Research Laboratory, Sensors Directorate, Wright Patterson AFB, OH, 45433 USA

a) Electronic Address: shin.mou.1@us.af.mil and adam.neal.3@us.af.mil

To fit the Hall data, first the temperature dependent carrier density is fit using the charge neutrality equation to make an initial guess at the concentrations and energies of the donors and acceptors in the material:¹

$$N_c \mathcal{F}_{1/2} \left(\frac{E_f - E_c}{kT} \right) + \frac{N_{ac}}{1 + 2 \exp\left(\frac{E_{ac} - E_f}{kT}\right)} = \frac{N_{dn}}{1 + 2 \exp\left(\frac{E_f - E_{dn}}{kT}\right)} \quad (\text{S1})$$

N_c is the conduction band effective density of states, N_{ac} the acceptor concentration, N_{dn} the donor concentration, E_{ac} the acceptor energy, E_{dn} the donor energy, and $\mathcal{F}_{1/2}$ the normalized Fermi-Dirac integral of order one half. N_c is calculated analytically¹ using an electron effective mass of $0.3m_o$.²⁻⁴ With this initial fitting, we can then calculate the temperature dependent conduction band carrier density, the temperature dependent ionized impurity density, and the temperature dependent neutral impurity density. Next, those temperature dependent quantities are input into the appropriate models for ionized impurity scattering, neutral impurity scattering, and polar optical phonon scattering rates in Ga₂O₃. The scattering rate due to ionized impurities is:⁵

$$\frac{1}{\tau_{II}} = \frac{N_I q^4}{16\sqrt{2}m_*\pi\kappa_S^2\varepsilon_0^2} \left[\ln(1 + \gamma^2) - \frac{\gamma^2}{1+\gamma^2} \right] E^{-3/2} \quad (S2)$$

$$\gamma^2 = \frac{8m_*EL_D^2}{\hbar^2} \quad (S3)$$

where m_* is the electron effective mass, κ_S the relative dielectric constant, and L_D the Debye length due to screening of ionized impurities by conduction band free electrons. The neutral impurity scattering rate is:⁶

$$\frac{1}{\tau_{ni}} = \frac{(4\pi)(20)\kappa_S\varepsilon_0N_{ni}\hbar^3}{m_*^2q^2} \quad (S4)$$

And the polar optical phonon scattering rate is:⁷

$$\frac{1}{\tau_{POP}} = \frac{q^2\omega_o\left(\frac{\kappa_S}{\kappa_\infty}-1\right)}{4\pi\kappa_S\varepsilon_0\hbar\sqrt{2[E/m_*]}} \left[N_o\sqrt{1+\frac{\hbar\omega_o}{E}} + (N_o+1)\sqrt{1-\frac{\hbar\omega_o}{E}} - \frac{\hbar\omega_o N_o}{E} \sinh^{-1}\left(\frac{E}{\hbar\omega_o}\right)^{1/2} + \frac{\hbar\omega_o(N_o+1)}{E} \sinh^{-1}\left(\frac{E}{\hbar\omega_o}-1\right)^{1/2} \right] \quad (S5)$$

$$N_o = \frac{M}{e^{\hbar\omega_o/kT}-1} \quad (S6)$$

where $\kappa_S = 10$ is the low frequency relative dielectric constant,^{8,9} $\kappa_\infty = 3.5$ the high frequency relative dielectric constant,⁹⁻¹¹ $\hbar\omega_o = 44$ meV the effective phonon energy,¹² and $M = 1.5$ the effective number of phonon modes. The total scattering rate is the sum $\tau_m^{-1} = \tau_{ni}^{-1} + \tau_{POP}^{-1} + \tau_{II}^{-1}$. Using these scattering rates, the Hall mobility and Hall factor can be calculated as:^{13,14}

$$\mu_h = r_h \frac{q\langle\tau_m\rangle}{m_*} \quad (S7)$$

$$r_h = \frac{\langle\tau_m^2\rangle}{\langle\tau_m\rangle^2} \quad (S8)$$

$$\langle\tau_m\rangle = \frac{\int_0^\infty E^{3/2}\tau_m(E)f(E) dE}{\int_0^\infty E^{3/2}f(E) dE} \quad (S9)$$

where $\langle\tau_m\rangle$ is the average momentum relaxation time, averaged over energy as shown. Finally, with the Hall factor r_h , the Hall carrier density can be calculated as:

$$n_h = \frac{n}{r_h} \quad (\text{S10})$$

and the temperature dependent carrier density can be fit while including the effect of the Hall factor. By iterating between fitting the temperature dependent Hall carrier density, fitting the temperature dependent mobility, and calculating the Hall factor, a simultaneous, self-consistent fit of the Hall effect data is achieved.

Supplementary References

- ¹ S.M. Sze and K.K. Ng, *Physics of Semiconductor Devices, 3rd ed.* (John Wiley & Sons, 2007) pp. 17-27
- ² H. He, R. Orlando, M.A. Blanco, R. Pandey, E. Amzallag, I. Baraille, and M. Rérat, *Phys. Rev. B* **74**, 195123 (2006).
- ³ H. Peelaers and C.G. Van de Walle, *Phys. Status Solidi B* **252**, 828 (2015).
- ⁴ J. Furthmüller and F. Bechstedt, *Phys. Rev. B* **93**, 115204 (2016).
- ⁵ M. Lundstrom, *Fundamentals of Carrier Transport 2nd ed.* (Cambridge University Press, New York, 2000) p. 70
- ⁶ C. Erginsoy, *Phys. Rev.* **79**, 1013 (1950).
- ⁷ M. Lundstrom, *Fundamentals of Carrier Transport 2nd ed.* (Cambridge University Press, New York, 2000) p. 86
- ⁸ B. Hoeneisen, C.A. Mead, and M.A. Nicolet, *Solid-State Electron.* **14**, 1057 (1971).
- ⁹ M. Schubert, R. Korlacki, S. Knight, T. Hofmann, S. Schöche, V. Darakchieva, E. Janzén, B. Monemar, D. Gogova, Q.-T. Thieu, R. Togashi, H. Murakami, Y. Kumagai, K. Goto, A. Kuramata, S. Yamakoshi, and M. Higashiwaki, *Phys. Rev. B* **93**, 125209 (2016).
- ¹⁰ M. Rebien, W. Henrion, M. Hong, J.P. Mannaerts, and M. Fleischer, *Appl. Phys. Lett.* **81**, 250 (2002).
- ¹¹ C. Sturm, J. Furthmüller, F. Bechstedt, R. Schmidt-Grund, and M. Grundmann, *APL Mater.* **3**, 106106 (2015).
- ¹² N. Ma, N. Tanen, A. Verma, Z. Guo, T. Luo, H.G. Xing, and D. Jenna, *Appl. Phys. Lett.* **109**, 212101 (2016).
- ¹³ M. Lundstrom, *Fundamentals of Carrier Transport 2nd ed.* (Cambridge University Press, New York, 2000) pp. 136-137
- ¹⁴ M. Lundstrom, *Fundamentals of Carrier Transport 2nd ed.* (Cambridge University Press, New York, 2000) p. 171